Available online at www.sciencedirect.com
SCIENCE DIRECT®
Optics Communications 246 (2005) 97–105
OPTICS COMMUNICATIONS
www.elsevier.com/locate/optcom

Optical trapping of a spherically symmetric rayleigh sphere: a model for optical tweezers upon cells

Yi-Ren Chang [a,*], Long Hsu [b], Sien Chi [a,c]

[a] Department of Photonics and Institute of Electro-Optical Engineering, National Chiao Tung University, 1001 Ta Hsueh Road, Hsinchu 300, Taiwan, ROC
[b] Department of Electrophysics, National Chiao Tung University, 1001 Ta Hsueh Road, Hsinchu 300, Taiwan, ROC
[c] Department of Electrical Engineering, Yuan Ze University, 135, Far-East Road, Chung-Li, Taoyuan, Taiwan, ROC

Received 8 July 2004; received in revised form 4 October 2004; accepted 25 October 2004

Abstract

Optical tweezers have become a popular manipulation and force measurement tool in cellular and molecular biology. However, there is still a lack of a sophisticated model for optical tweezers on trapping cells. In this paper, we present a novel model for optical tweezers to calculate the stiffness of trapping force upon a spherically symmetric Rayleigh sphere, which stimulates a common biological cell. A numerical simulation of this model shows that the stiffness of an optical tweezers system in trapping a cell is significantly smaller than that in trapping a polystyrene bead of the same size. Furthermore, under a small variant condition of the refractive index, the proposed model provides an approximate method which requires only the radial distribution of the trapped cell's refractive index for calculating the stiffness.

PACS: 42.25.Fx; 42.50.Vk
Keywords: Optical tweezers; Rayleigh scattering; Biophotonics

1. Introduction

Since Ashkin et al. [1] first trapped a micron size bead with a focused laser beam in 1986, optical tweezers have become a popular tool for manipulation [2–5] and force measurement in cellular and molecular biology [6–9]. Up to now, there are two major models describing the trapping mechanism of optical tweezers; namely, a ray-optics (RO) model by Ashkin [10] and an electromagnetics (EM) model by Harada and Asakura [11]. The RO model is valid as the radius of the trapped particle is larger than ten

* Corresponding author. Tel. +8863571212156165; fax: +88635725230.
E-mail address: YRChang.eo91g@nctu.edu.tw (Y.-R. Chang).

0030-4018/$ - see front matter © 2004 Elsevier B.V. All rights reserved.
doi:10.1016/j.optcom.2004.10.066

times the wavelength of the laser. However, the EM model is valid as the radius of the trapped particle is much smaller than the wavelength of the laser. Although there are some other models dealing with particle whose radius is near the wavelength of the laser [12–14], all the mentioned models assume that the trapped particle has a uniform refractive index. Unfortunately, this assumption is not true for biological cells. Therefore, it is desired to have a sophisticated model for optical tweezers on trapping a non-uniform particle like organelles and cells.

In this work, we assume the non-uniform particle as a small Rayleigh sphere with spherically symmetric refractive index. To be more specific, we assume that this sphere is composed of multiple concentric layers with different refractive indices. In this regard, as the thickness of each layer approaches infinitely small and the variation of the refractive indices of adjacent layers is small enough, the structure of this spherically symmetric Rayleigh sphere could be analogous to that of the common biological cells.

In Section 2, we first solve for the electric potential of the proposed cell-like sphere of multiple concentric layers in a laser beam. Under the small variant condition of the refractive indices of adjacent layers as mentioned above, it can be shown that such a cell-like sphere functions as a single effective electric dipole induced by the surrounding electric field. Then, in Section 3, substituting the induced electric dipole moment into Harada and Asakura's EM model, we obtain a trapping force produced by an optical tweezers system upon the cell-like sphere. Lastly, in Section 4, we will compare the difference in magnitude between the trapping force upon a uniform sphere and that upon a non-uniform cell of the same size. In this exercise, a Chinese hamster ovary (CHO) cell at an artificially reduced size is used as an example of the non-uniform cell. The same reduced-size CHO cell but of an artificially single uniform layer, a silica bead and a polystyrene bead are used as the uniform sphere, separately. The selection of the four samples is simply due to the availability of the information on their structures and distributions of refractive indices.

2. Theoretical analysis

2.1. Electric dipole moment of a spherically symmetric sphere

To illustrate the induced electric dipole moment of a cell-like sphere by the electric field of a focused laser beam, we consider in Fig. 1(a), N-layer sphere of radius R in an electric field E_o. Suppose that the radius r_k and the index of refraction n_k of each concentric layer is known, where the subscript k refers to the kth layer. For simplicity, we assume the cell-like sphere a Rayleigh particle, which means that it is such a very small particle that the electric field around it is nearly unchanged. As shown in Fig. 1, the electric field outside the sphere is assumed $\vec{E}_o = \hat{z}E_o + \Delta\vec{E}_o \approx \hat{z}E_o$, where E_o is the average amplitude of the electric field, and ΔE_o is a variation term.

It can be shown that the electric potential Φ_k of the kth layer of the multi-layer sphere for $r_{k-1} < r < r_k$ is usually given in the general form [15]

$$\Phi_k(r,\theta) = \sum_{l=0}^{\infty} \left[A_{l,k} r^l + B_{l,k} r^{-(l+1)}\right] P_l(\cos\theta), \qquad (1)$$

where r and θ are of spherical coordinates, $A_{l,k}$ and $B_{l,k}$ are two coefficients, and $P_l(\cos\theta)$ is the Legendre polynomial of order l. Here, in our case, many of the coefficients $A_{l,k}$ and $B_{l,k}$ would vanish. Firstly, as r approaches infinity, the boundary condition $\Phi_{N+1}(r \to \infty) = -E_o z = -E_o r P_1(\cos\theta)$ leads to the vanishment of all coefficients $A_{l,N+1}$ except for $A_{1,N+1} = -E_o$. Secondly, as r ap-

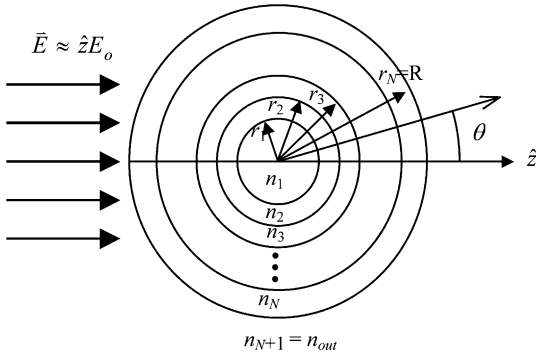

Fig. 1. The structure of the proposed multi-layer spherically symmetric Rayleigh sphere.

proaches the origin, $B_{l,1} = 0$ because the potential near the center of the sphere must be finite within the first layer where $k = 1$. Finally, the rest of the coefficients are left to be determined according to the following boundary conditions:

$$-\frac{1}{r_k}\frac{\partial \Phi_k}{\partial \theta}\bigg|_{r=r_k} = -\frac{1}{r_k}\frac{\partial \Phi_{k+1}}{\partial \theta}\bigg|_{r=r_k} \tag{2}$$

and

$$-n_k^2\frac{1}{r_k}\frac{\partial \Phi_k}{\partial r}\bigg|_{r=r_k} = -n_{k+1}^2\frac{\partial \Phi_{k+1}}{\partial r}\bigg|_{r=r_k}. \tag{3}$$

Substituting Eq. (1) for $\Phi_{N+1}(r,\theta)$ into Eqs. (2) and (3), we obtain

$$A_{l,k} + B_{l,k}/r_k^{2l+1} = A_{l,k+1} + B_{l,k+1}/r_k^{2l+1} \tag{4}$$

and

$$\left(\frac{n_k}{n_{k+1}}\right)^2 lA_{l,k} - \left(\frac{n_k}{n_{k+1}}\right)^2 (l+1)B_{l,k}/r_k^{2l+1} = lA_{l,k+1} - (l+1)B_{l,k+1}/r_k^{2l+1}. \tag{5}$$

From Eqs. (4) and (5), we can relate the coefficients $A_{l,N+1}(=-E_o)$ and $B_{l,N+1}$ of the space outside the sphere to the coefficients $A_{l,1}$ and $B_{l,1}(=0)$ of the first layer inside the sphere as below.

For $l = 1$, we have

$$\begin{bmatrix} -E_0 \\ B_{l,N+1} \end{bmatrix} = \begin{bmatrix} \frac{2+m_N^2}{3} & \frac{2(1-m_N^2)}{3r_N^3} \\ \frac{(1-m_N^2)r_N^3}{3} & \frac{1+2m_N^2}{3} \end{bmatrix} \cdot \cdots \cdot \begin{bmatrix} \frac{2+m_2^2}{3} & \frac{2(1-m_2^2)}{3r_2^3} \\ \frac{(1-m_2^2)r_2^3}{3} & \frac{1+2m_2^2}{3} \end{bmatrix} \cdot \begin{bmatrix} \frac{2+m_1^2}{3} & \frac{2(1-m_1^2)}{3r_1^3} \\ \frac{(1-m_1^2)r_1^3}{3} & \frac{1+2m_1^2}{3} \end{bmatrix} \cdot \begin{bmatrix} A_{1,1} \\ 0 \end{bmatrix} = \begin{bmatrix} M_{11} & M_{12} \\ M_{21} & M_{22} \end{bmatrix} \cdot \begin{bmatrix} A_{1,1} \\ 0 \end{bmatrix}, \tag{6}$$

where $m_k \equiv n_k/n_{k+1}$ and the matrix of M_{11}, M_{12}, M_{21}, and M_{22} results from the $N-1$ inner products of N interface matrices of various functions of m_k.

Similarly, for $l \neq 1$, we have

$$\begin{bmatrix} 0 \\ B_{l,N+1} \end{bmatrix} = \begin{bmatrix} \frac{l+1+lm_N^2}{2l+1} & \frac{(l+1)(1-m_N^2)}{(2l+1)r_N^{2l+1}} \\ \frac{(l-m_N^2)r_N^{2l+1}}{2l+1} & \frac{l+l(l+1)m_N^2}{2l+1} \end{bmatrix} \cdot \cdots \cdot \begin{bmatrix} \frac{l+1+lm_2^2}{2l+1} & \frac{(l+1)(1-m_2^2)}{(2l+1)r_2^{2l+1}} \\ \frac{(l-m_2^2)r_2^{2l+1}}{2l+1} & \frac{l+l(l+1)m_2^2}{2l+1} \end{bmatrix} \cdot \begin{bmatrix} \frac{l+1+lm_1^2}{2l+1} & \frac{(l+1)(1-m_1^2)}{(2l+1)r_1^{2l+1}} \\ \frac{(l-m_1^2)r_1^{2l+1}}{2l+1} & \frac{l+l(l+1)m_1^2}{2l+1} \end{bmatrix} \cdot \begin{bmatrix} A_{1,1} \\ 0 \end{bmatrix}. \tag{7}$$

Eq. (7) reveals that all $A_{l,k}$ and $B_{l,k}$ vanish for $l \neq 1$. This leads to a simplified form for the electric potential outside the sphere, $\Phi_{N+1}(r,\theta) = -E_o z + B_{1,N+1}\, z/r^3$, in which only the coefficient $B_{1,N+1}$ is left to be solved. Eq. (6) indicates that $B_{1,N+1}$ and, thus, the electric potential outside the sphere, $\Phi_{N+1}(r,\theta)$, can be directly related to $A_{1,1}$ or $\Phi_1(r,\theta) = A_{11}z$ of the most inner layer via M_{11}, M_{12}, M_{21} and M_{22} as given by

$$\Phi_{N+1}(r,\theta) = -E_o r\cos\theta - E_o\frac{M_{21}\cos\theta}{M_{11}r^2}. \tag{8}$$

It can be seen that the overall electric potential outside the cell-like sphere is simply the sum of the electric potential of the originally applied field E_o and the electric potential of an electric dipole at the origin. Conventionally, the sphere is treated as a single effective electric dipole which is induced by the surrounding electric field. Classical electrodynamics tells us that this effective electric dipole will generate a dipole moment $p = 4\pi\varepsilon_{out}E_o(M_{21}/M_{11})$, where ε_{out} is the dielectric constant of the medium outside the sphere. This results in an effective polarizability $\alpha = p/(\varepsilon_{out}E_o)$ for the cell-like sphere, as given by

$$\alpha = -4\pi M_{21}/M_{11}. \tag{9}$$

It is worth to point out that the availability of this effective polarizability for a cell-like sphere is due to the analogy between a cell and a spherically symmetric multi-layer sphere. As will be seen in the following section, this effective polarizability α is a key factor in deriving the trapping force produced by an optical tweezers system upon a

cell-like sphere. Yet the calculation for α is still difficult, because it is complicated to calculate for the matrix elements M_{11}, M_{12}, M_{21}, and M_{22} According to Eq. (6), calculating for the matrix elements requires a series of inner production of the interface matrices of the N layers, involving various functions of different m_k, as shown above.

To overcome this problem, we further develop an approximate method for calculating α by applying a small variant condition of the refractive indices of adjacent layers. For this purpose, we assume that the thickness of each layer, $R/(N-1)$, approaches infinitely small, which implies $N \to \infty$. Under this condition, the structure of such a Rayleigh sphere of infinitely multiple layers could be analogous to that of a common cell. Consequently, it can be shown that the four elements M_{11}, M_{12}, M_{21}, and M_{22} are simplified in the approximate forms of

$$\begin{aligned} M_{11} &\approx 1+\frac{2}{3}\cdot\lim_{N\to\infty}\sum_{k=1}^{N}\mathrm{d}m_k \\ &= 1+\frac{2}{3}\cdot\lim_{N\to\infty}\sum_{k=1}^{N}\frac{1}{n(k\ R/N)} \\ &\quad\cdot\frac{n(k\ R/N)-n((k+1)R/N)}{R/N}\cdot\frac{R}{N} \\ &= 1+\frac{2}{3}\cdot\ln[n(0)/n(R)], \end{aligned} \tag{10}$$

$$\begin{aligned} M_{12} &\approx -\frac{4}{3}\cdot\lim_{N\to\infty}\sum_{k=1}^{N}\mathrm{d}m_k/r_k^3 \\ &= \frac{4}{3}\cdot\int_0^R\frac{n'(r')}{n(r')\cdot r'^3}\,\mathrm{d}r', \end{aligned} \tag{11}$$

$$\begin{aligned} M_{21} &\approx -\frac{2}{3}\cdot\lim_{N\to\infty}\sum_{k=1}^{N}\mathrm{d}m_k r_k^3 \\ &= \frac{2}{3}\cdot\int_0^R\frac{n'(r').r'^3}{n(r')}\,\mathrm{d}r', \end{aligned} \tag{12}$$

and

$$\begin{aligned} M_{22} &\approx 1+\frac{4}{3}\cdot\lim_{N\to\infty}\sum_{k=1}^{N}\mathrm{d}m_k \\ &= 1+\frac{4}{3}\cdot\ln[n(0)/n(R)], \end{aligned} \tag{13}$$

where $n(0)$ and $n(R)$ are the refractive indices of the layers at the center and the edge of the cell-like sphere, respectively.

Substituting Eqs. (10)–(13) into Eq. (6), we may rewrite the coefficient $A_{1,1}$ and $B_{1,N+1}$ in terms of the electric field outside the sphere, E_o, and the radial distribution of the refractive indices of the sphere, $n(r)$, as given by

$$A_{1,1} \approx -E_o \Big/ \left(1+\frac{2}{3}\cdot\ln[n(0)/n(R)]\right) \tag{14}$$

and

$$B_{1,N+1} \approx -E_o\frac{\frac{2}{3}\cdot\int_0^R\frac{n'(r')\cdot r'^3}{n(r')}\,\mathrm{d}r'}{1+\frac{2}{3}\cdot\ln[n(0)/n(R)]}. \tag{15}$$

As a result, the electric potential outside the sphere is approximately in the form of

$$\begin{aligned} \Phi(r) &\approx -E_o r\cos\theta - E_o \\ &\quad\cdot\frac{\frac{2}{3}\cdot\int_0^R\frac{n'(r')\cdot r'^3}{n(r')}\,\mathrm{d}r'}{1+\frac{2}{3}\cdot\ln[n(0)/n(R)]}\cdot\frac{1}{r^2}cos\theta. \end{aligned} \tag{16}$$

Consequently, the dipole moment p of the effective electric dipole is given by

$$\begin{aligned} p &= 4\pi\varepsilon_{out}B_1(R) \\ &\approx 4\pi\varepsilon_{out}E_o\cdot\frac{\frac{2}{3}\cdot\int_R^0\frac{n'(r')\cdot r'^3}{n(r')}\,\mathrm{d}r'}{1+\frac{2}{3}\cdot\ln[n(0)/n(R)]}. \end{aligned} \tag{17}$$

And the effective polarizability α of the cell-like sphere is approximated as given by

$$\alpha \approx \frac{8\pi}{3}\cdot\frac{\int_R^0\frac{n'(r')\cdot r'^3}{n(r')}\,\mathrm{d}r'}{1+\frac{2}{3}\cdot\ln[n(0)/n(R)]}. \tag{18}$$

Eq. (18) signifies that only the radial distribution of the refractive index $n(r)$ of a cell is required for α. Obviously, the calculation for α becomes simple under the small variant condition of refractive index. As will be shown in the following section, this approximate method for calculating α also simplifies the calculation for the trapping force produced by an optical tweezers system upon a spherical cell.

2.2. Light force

In the preceding section, we propose a Rayleigh sphere of multiple concentric layers to simulate a

common biological cell. In addition, we have proved that such a cell-like Rayleigh sphere is equivalent to a single effective electric dipole. This model enables us to further derive the trapping force induced by an optical tweezers system upon the cell-like sphere. This is done by substituting into Harada and Asakura's model the dipole moment $\vec{p}$ of this effective electric dipole, which is induced in a focused laser beam of wavelength λ, as shown in Fig. 2.

It can be shown that an electric dipole moment induced in a non-uniform electric field will experience a trapping force produced by the focused laser beam due to a gradient dipole force [11]

$$\vec{\mathbf{F}}_{\text{grad}}(\vec{\mathbf{r}}) = [\vec{\mathbf{p}}(\vec{\mathbf{r}}) \cdot \vec{\nabla}]\,\vec{\mathbf{E}}(\vec{\mathbf{r}}) = \frac{\alpha}{2} \cdot \frac{n_{\text{out}}}{c}\,\vec{\nabla} I(\vec{\mathbf{r}}), \quad (19)$$

in which α is the effective polarizability of the cell-like sphere as given in Eq. (18), n_{out} is the refractive index of the medium surrounding the sphere, c is the speed of light in vacuum, and $I(\vec{\mathbf{r}})$ is the intensity distribution of the focused laser beam. Substituting for α from Eqs. (18) and (19) for the gradient dipole force $\vec{\mathbf{F}}_{\text{grad}}(\vec{\mathbf{r}})$ can be rewritten in the form

$$\vec{\mathbf{F}}_{\text{grad}}(\vec{\mathbf{r}}) \approx \frac{4\pi n_{\text{out}}}{3c} \cdot \frac{\int_0^R \frac{n'(r')\cdot r'^3}{n(r')}\,\mathrm{d}r'}{1 + \frac{2}{3}\cdot \ln[n(0)/n(R)]}\,\vec{\nabla} I(\vec{\mathbf{r}}). \quad (20)$$

Similar to Harada and Asakura's EM model, we also consider a Gaussian laser beam of intensity as given by

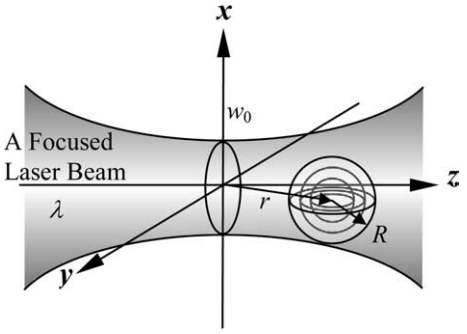

Fig. 2. The schematic of a Rayleigh sphere in a non-uniform electric field.

$$I(\vec{\mathbf{r}}) = \left(\frac{2P}{\pi w_0}\right) \frac{1}{1 + (2\tilde{z}/kw_{\text{o}})^2} \exp\left[-\frac{2(\tilde{x}^2 + \tilde{y}^2)}{1 + (2\tilde{z}/kw_0)^2}\right], \quad (21)$$

where P, w_0, $k = 2\pi/\lambda$ are the power, the beam waist, and the wave number of the laser beam, respectively. And $(\tilde{x}, \tilde{y}, \tilde{z}) = (x/w_0, y/w_0, z/w_{\text{o}})$ are the normalized coordinates with respect to w_0 Substituting for $I(\vec{\mathbf{r}})$ from Eq. (21), the gradient dipole force $\vec{\mathbf{F}}_{\text{grad}}(\vec{\mathbf{r}})$ in Eq. (20) can be decomposed into the following three components:

$$\vec{\mathbf{F}}_{\text{grad},x}(\vec{\mathbf{r}}) = -\hat{x}\frac{\alpha n_{\text{out}}}{c}\left(\frac{P}{\pi w_0^2}\right) \frac{4\tilde{x}/w_0}{[1 + (2\tilde{z}/kw_0)^2]^2} \times \exp\left[-\frac{2(\tilde{x}^2 + \tilde{y}^2)}{1 + (2\tilde{z}/kw_0)^2}\right], \quad (22)$$

$$\vec{\mathbf{F}}_{\text{grad},y}(\vec{\mathbf{r}}) = -\hat{y}\frac{\alpha n_{\text{out}}}{c}\left(\frac{P}{\pi w_0^2}\right) \frac{4\tilde{y}/w_0}{[1 + (2\tilde{z}/kw_0)^2]^2} \times \exp\left[-\frac{2(\tilde{x}^2 + \tilde{y}^2)}{1 + (2\tilde{z}/kw_0)^2}\right], \quad (23)$$

and

$$\vec{\mathbf{F}}_{\text{grad},z}(\vec{\mathbf{r}}) = -\hat{z}\frac{\alpha n_{\text{out}}}{c}\left(\frac{P}{\pi w_0^2}\right) \frac{16\tilde{z}/k^2 w_0^3}{[1 + (2\tilde{z}/kw_0)^2]^2} \times \left[1 - \frac{2(\tilde{x}^2 + \tilde{y}^2)}{1 + (2\tilde{z}/kw_0)^2}\right] \times \exp\left[-\frac{2(\tilde{x}^2 + \tilde{y}^2)}{1 + (2\tilde{z}/kw_0)^2}\right]. \quad (24)$$

Conventionally, optical tweezers are analogous to a three-dimensional optical spring. This is easily seen from Eqs. (22)–(24) that, to the first order approximation, each component of the trapping force is linearly proportional to its corresponding coordinate, which is indeed the displacement from the center of the trapped sphere to the center of the laser beam waist. Therefore, the three components of the stiffness of the 3-D optical spring are given by

$$k_x = k_y = \frac{4\alpha n_{\text{out}}}{c}\left(\frac{P}{\pi w_0^4}\right) \quad (25)$$

and

$$k_z = \frac{16\alpha n_{\text{out}}}{c}\left(\frac{P}{\pi k^2 w_0^6}\right). \tag{26}$$

Obviously, both the trapping force itself and the stiffness of the trapping force are linearly proportional to the induced palrizability α.

By the way, in addition to the gradient dipole force, there is an undesired scattering force exerted on the cell-like Rayleigh sphere. Essentially, the scattering force corresponds to a radiative-damping force. This results from the emission of electromagnetic radiation by the accelerating effective electric dipole, acting as an antenna, in the oscillating electric field of the laser beam. According to the antenna theory, the scattering force is along the Poynting vector of the laser beam as given by

$$\begin{aligned}\vec{\mathbf{F}}_{\text{scat}}(\vec{\mathbf{R}}) &= \hat{z}(8\pi^3/3)I\alpha^2 \cdot n_{\text{out}}/c \\ &\approx \hat{z}\frac{512\pi^5 n_{\text{out}}}{27c}\left[\frac{\int_R^0 \frac{n'(r')\cdot r'^3}{n(r')}\,\mathrm{d}r'}{1+\frac{2}{3}\cdot\ln[n(0)/n(R)]}\right]^2 \\ &\quad\times\left(\frac{2P}{\pi w_0}\right)\frac{1}{1+(2\tilde{z}/kw_0)^2} \\ &\quad\times\exp\left[-\frac{2(\tilde{x}+\tilde{y}^2)}{1+(2\tilde{z}/kw_0)^2}\right].\end{aligned} \tag{27}$$

After all, the total light force $\vec{\mathbf{F}}_{\text{tot}}$ exerted on the cell-like Rayleigh sphere is the sum of the gradient dipole force $\mathbf{F}_{\text{grad}}$ and the scattering force $\mathbf{F}_{\text{scat}}$.

3. Numerical results

3.1. Data of refractive indices and sizes of Chinese hamster ovary cell

Practically, detailed refractive indices of organelles and bacterial cells are rarely characterized. Here, we only find a rough estimate on the refractive index of mammalian cells in Brunsting and Mullaney's work [16]. They modeled the CHO cell as a coated sphere in an optical and morphological fashion. In their model, the nucleus of the mammalian suspension cell is surrounded by its cytoplasm.

On one hand, the magnitudes of the refractive index of the cytoplasm, n_{cyt} and the refractive index of the nucleus, n_{nuc} were measured to be 1.3703 and 1.392 ± 0.005, respectively. On the other hand, they found a linear relationship between the radius of the nucleus, r_{nuc} and the radius of the cell, R, for many CHO cells of various sizes as given by

$$R = (1.38 \pm 0.02)r_{\text{nuc}} + (0.03 \pm 0.05). \tag{28}$$

In average, the magnitudes of $\langle r_{\text{nuc}}\rangle$ and $\langle R\rangle$ were measured to be 8.1 ± 0.9 and 11.2 ± 0.5 μm, respectively.

Unfortunately, the sizes of CHO cell and even mammalian cells are too large to fit in Rayleigh regime. However, these data are still meaningful in the following simulation in Section 3.2 for two artificially reduced-size CHO cells for comparison. Here, we take an artificial CHO cell at a reduced size with a radius of $R = 50$ nm as an example to our cell-like model. A similar assumption was once adopted in [17]. According to Eq. (28), this suggests that the radius of its nuclear is approximately $r_{\text{nuc}} = 36.2 \pm 0.5$ nm. Presumably, we further assume the radial distribution of refractive index of this artificial CHO cell as given by

$$n(r) = \begin{cases} 1.392 \pm 0.005 & \text{for } 0 \leqslant r < r_{\text{nuc}} \quad \text{(cytoplasm)} \\ 1.3703 & \text{for } r_{\text{nuc}} \leqslant r \leqslant R \quad \text{(nuclear)}. \end{cases} \tag{29}$$

In this regard, $n(0) = 1.392 \pm 0.005$ and $n(R) = 1.3703$.

Then, we take another CHO cell at the same reduced size but of an artificially uniform refractive index of 1.379 as an example of uniform sphere to our cell-like model. Note that the value of 1.379 is the averaged refractive index of the CHO cell.

3.2. Numerical analysis

The validity of our model is numerically examined by comparing the difference in magnitude between the effective polarizabilities α of the trapped samples as well as the resulting stiffnesses k of optical tweezers for a uniform sphere and those for a non-uniform cell of the same size. In this exercise, other than the uniform artificial CHO cell, a silica

bead and a polystyrene bead are also ideal to be used as the uniform sphere, because they are often used in cellular and molecular biology experiments with optical tweezers. And the non-uniform artificial CHO cell seems an adequate example of the non-uniform cell. Surely, the radii of the two beads are taken to be the same as that of the two artificial CHO cells, which is 50 nm. Note that the refractive indices of uniform silica bead and polystyrene bead are 1.45 and 1.56, respectively. The samples are trapped in water, whose refractive index is 1.33. Additionally, the optical tweezers system is assumed consisting of a 10-mW Nd:YAG laser at a wavelength of $\lambda = 1064$ nm and a microscope objective of N.A. = 1.25.

On the one hand, by substituting the appropriate values into Eqs. (9) and (18) for the effective polarizabilities of the non-uniform artificial CHO cell of 50 nm in radius, we obtain an exact solution, $\alpha_{\text{non-uni-CHO,exact}} = (3.798 \pm 0.263) \times 10^{-23}$ m^3, and an approximate solution, $\alpha_{\text{non-uni-CHO,appr}} = (3.691 \pm 0.221) \times 10^{-23}$ m^3, separately. Similarly, we obtain, $\alpha_{\text{uni-CHO}} = 3.833 \times 10^{-23}$ m^3, $\alpha_{\text{silica}} = 9.291 \times 10^{-23}$ m^3 and $\alpha_{\text{poly}} = 17.48 \times 10^{-23}$ m^3 for the uniform artificial CHO cell, the silica bead and the polystyrene bead, respectively.

On the other hand, by substituting the appropriate values into Eqs. (25) and (26), we obtain the values of the transverse and the longitudinal components of the optical tweezers' stiffness resulting from the effective polarizabilities, as given above. All data for the two kinds of artificial CHO cells, the silica bead, and the polystyrene bead are listed in Table 1.

Table 1
Numerical result of effective polarizabilities and stiffness

	Non-uniform artificial CHO cell		Uniform artificial CHO cell	Silica bead	Polystyrene bead
	Accurate result (matrix calculation)	Approximate result (small variant condition)			
Refractive index	$n_{\text{nuc}} = 1.392 \pm 0.005$ ($0 \leqslant r < 36.2$ nm) $n_{\text{cyt}} = 1.3703$ (36.2 nm $\leqslant r \leqslant 50$ nm)		1.379	1.45	1.56
Polarizability (10^{-23} m^3)	3.798 ± 0.263	3.691 ± 0.221	3.833	9.291	17.48
Transverse stiffness, k_x and k_y (10^{-9} N/m)	9.426 ± 0.653	9.359 ± 0.548	9.514	23.06	43.39
Longitudinal stiffness, k_z (10^{-9} N/m)	0.5668 ± 0.0393	0.5627 ± 0.0330	0.5721	1.387	2.609

The effective polarizabilities of four 50-nm-in-radius samples: including a non-uniform artificial CHO cell, a uniform artificial CHO cell, a silica bead, and a polystyrene bead, which are followed by their corresponding transverse and longitudinal components of the resulting stiffness of an optical tweezers system using a 10-mW Nd:YAG laser at a wavelength of $\lambda = 1064$ nm.

4. Discussion

From Table 1, it can be seen that the effective polarizabilities α and the three components of the optical tweezers' stiffness k of a silica bead and of a polystyrene bead are about 2.5–4.5 times those of either artificial CHO cell. The difference in α and k between the beads and the artificial CHO cells mainly results from the difference in the refractive indices between them. According to Eq. (20), this relationship should be applicable to the trapping forces, the gradient dipole forces pro-

duced by the optical tweezers upon them. This predication somehow agrees with the experimental result in Liang et al.'s work [18]. They found that the trapping force upon a polystyrene bead is three to four times that upon an *Escherichia coli* cell. Similarly, we also found in our measurement that the trapping force upon a 1-μm-in-diameter polystyrene bead is approximately 3.8 times that upon a *Klebsiella pneumoniane* cell whose long axis is 1.2 μm and short axis is 0.98 μm. It is worth to note that even the sizes and shapes of the uniform bead and the *K. pneumoniane* cell are not really in the Rayleigh regime, similar relationship of the trapping forces between them remains the same.

In general, it seems that the larger the refractive index is, the larger the corresponding α, k, and trapping force are. However, on the contrary, the uniform artificial CHO cell gives rise to a slightly larger α and k than the non-uniform artificial CHO cell of the same size, as shown in Table 1. Note that the refractive index of the former is only the average of that of the latter. Most importantly, this particular case emphasizes the dependence of trapping force upon the distribution of refractive index of the trapped cell.

Moreover, we see that the exact solution 3.798 ± 0.263 and the approximate solution 3.691 ± 0.221 to the effective polarizability of the non-uniform artificial CHO cell are nearly the same, only differing by 2.5%. This proves the validity of the approximate method in our model for the effective polarizability under the small variant condition of the refractive index.

5. Conclusion

As a summary, we have successfully developed a model to simulate a common biological cell as a spherically symmetrical Rayleigh sphere. This model is an extension of Harada and Asakura's EM model from a uniform sphere to a non-uniform cell. In this model, only the radial distribution of the refractive index of a cell is required for the following calculations: the effective polarizability of the cell, the resulting trapping force produced by an optical tweezers system upon the trapped cell, and the stiffness of the optical tweezers.

The numerical simulation of this model analytically predicts a three- to fivefold difference in trapping forces between an artificial CHO cell at a reduced size and a commonly used bead of the same size, which is mostly due to the difference in refractive index. On the one hand, the trapping force is dependent upon the distribution of refractive index of the trapped cell. The exact value of the trapping force can be derived by applying the accurate method of this model, which requires a series of matrix calculation. On the other hand, it is simple and convenient to estimate the trapping force by applying the approximate method of this model under the small variant condition of refractive index. Additionally, it is appropriate as well to estimate the trapping force by approximating the trapped cell as a uniform cell with an effectively averaged refractive index of the cell.

References

[1] A. Ashkin, J.M. Dziedzic, J.E. Bjorkholm, S. Chu, Opt. Lett. 11 (1986) 288.
[2] S.C. Grover, A.G. Skirtach, R.C. Gauthier, C.P. Grover, J. Biomed. Opt. 6 (2001) 14.
[3] M. Ozkan, T. Pisanic, J. Scheel, C. Barlow, S. Esener, S.N. Bhatia, Langmuir 19 (2003) 1532.
[4] Y. Wakamoto, I. Inoue, H. Moriguchi, K. Yasuda, Fresen. J. Anal. Chem. 371 (2001) 276.
[5] M. Ozkan, M. Wang, C. Ozkan, R. Flynn, A. Birkbeck, S. Esener, Biomed. Microdev. 5 (2003) 61.
[6] C.G. Baumann, S.B. Smith, V.A. Bloomfield, C. Bustamante, Proc. Natl. Acad. Sci. USA 94 (1997) 6185.
[7] A.D. Mehta, M. Rief, J.A. Spudich, D.A. Smith, R.M. Simmons, Science 283 (1999) 1689.
[8] M.C. Williams, J.R. Wenner, I. Rouzina, V.A. Bloomfield, Biophys. J. 80 (2001) 1932.
[9] G. Hummer, A. Szabo, Proc. Natl. Acad. Sci. USA 98 (2001) 3658.
[10] A. Ashkin, Biophys. J. 61 (1992) 569.
[11] Y. Harada, T. Asakura, Opt. Commun. 124 (1996) 529.
[12] J.P. Barton, D.R. Alexander, S.A. Schaub, J. Appl. Phys. 66 (1989) 4594.
[13] F. Ren, G. Gre'han, G. Gouesbet, Opt. Commun. 108 (1994) 343.
[14] A. Rohrbach, E.H.K. Stelzer, J. Opt. Soc. Am. A 18 (2001) 839.
[15] J.D. Jackson, Classical Electrodynamics, Wiley, New York, 1999, p. 157.
[16] A. Brunsting, P.F. Mullaney, Biophys. J. 14 (1974) 439.

[17] A. Katz, A. Alimova, Min Xu, E. Rudolph, M.K. Shah, H.E. Savage, R.B. Rosen, S.A. McCormick, R.R. Alfano, IEEE Sel. Top. Quantum Electron. 9 (2003) 277.

[18] M.N. Liang, S.P. Smith, S.J. Metallo, I.S. Choi, M. Prentiss, G.M. Whitesides, Proc. Natl. Acad. Sci. USA 97 (2000) 13092.